Chalcogenides Letters Vol. 18, No. 9, September 2021, p. 505 - 512

GSH capped Cu-Zn-In-S quantum dots: one-pot aqueous synthesis and cell labeling applications

L. Zhang[a,*] , Y. Wan[a], Y. Wu[a], J. Wang[a], D. Xu[a], W. Duan[a], D. Chen[a], D. Liu[b]
[a]*College of Medical Technology, Qiqihar Medical University, Qiqihar, Heilongjiang 161006, China*
[b]*Communication and Electronic Engineering Institute, Qiqihar University, Qiqihar, Heilongjiang 161006, China*

We report a one-pot method to directly synthesize highly luminescent Cu-In-Zn-S quantum dots(CIZS QDs) in aqueous media by using bio-compatible glutathione (GSH) as capping ligand and stabilizer. The influences of various experimental variables, including reaction time, pH value, and precursor ratio, have been systematically investigated. As a result, the stable ternary CIZS QDs with good photoluminescence emission properties and narrow size distribution can be obtained. In addition, the obtained GSH capped CIZS QDs exhibited excellent optical performance and water stability. It is a promising fluorescent probe for biological labels due to the absence of toxic heavy metal ions.

(Received June 6, 2021; Accepted September 3, 2021)

Keywords: Aqueous synthesis, CIZS QDs, GSH capped, Photoluminescence

1. Introduction

Research on photoluminescent semiconductor quantum dots (QDs) have received considerable attentions owing to their potential applications as biological labels during the past two decades [1, 2]. Relevant studies have been focused on II–VI or IV–VI QDs such as CdTe, PbSe and CdSe which have high quantum yields and relatively strong photoluminescence (PL) emission[3-5]. Unfortunately, the toxicity of the Cd/Pb-based QDs limits their applications, especially in the biological field [6,7]. Although various protections employing ZnS, polymers, and other nontoxic shells have been developed, the leakage of Cd/Pb ions through the shell and the radicals derived from light irradiation could still be observed [8,9].

Therefore, heavy-metal-free QDs have been gaining increased attention[10,11]. For example, copper chalcogenide based QDs have recently been extensively investigated due to their low toxicity, including binary (e.g. $Cu_{2-x}S$, $Cu_{2-x}Se$) [12,13], ternary (e.g. $CuInS_2$, $CuInSe_2$ and $AgInS_2$) [14,15] and quaternary (e.g.CuInZnS, CuSnZnS) QDs[15,16]. Furthermore, quaternary CIZS QDs are developed based on the ternary $CuInS_2$ QDs, which have the larger Stokes shift, high molar extinction coefficient and no highly toxic elements. But there are many limitations about the existing synthesis of CIZS QDs. Firstly, most reports about quaternary CIZS QDs have been synthesized in complicated organometallic procedure with high reaction temperature and low efficiency[17-20]. Secondly, the as-prepared hydrophobic QDs in organic phase are poor

* Corresponding author: zhangliping1978@163.com
https://doi.org/10.15251/CL.2021.189.505

biocompatibility and high biotoxicity. The indispensable ligand exchange and surface modification can result in degradation of QDs photoluminescence performance. Therefore, it is necessary to develop a novel synthesis method to obtain hydrophilic and high quality color tunable CIZS QDs without any organometallic or toxic precursors, which hold enormous potential in biological analysis and optoelectronics applications. Therefore, the preparation of quaternary CIZS QDs with excellent properties attracts increasing attention.

In order to the above problem, we introduced a facile and green strategy for hydrophilic synthesis of CIZS QDs by using low reaction time and temperature (3 h, 120 °C). Compared with previous reports, our strategy only utilized GSH as the stabilizer and capping ligand for CIZS QDs. GSH capped QDs were considered more biocompatible as compared to other thiol capping ligands[21, 22]. The optimization of all experimental parameters including reaction time, pH value, and precursors concentration were carried out. The prepared CIZS QDs were highly biocompatible and showed specific red fluorescence bioimaging of MDA-MB-231 cells.

2. Experimental details

2.1. Chemicals

$CuCl_2 \cdot 2H_2O$(AR), $InCl_3 \cdot 4H_2O$(98%), $Zn(AC)_2 \cdot 2H_2O$(99.0%), C_2H_5NS (≥98.0%),and GSH(98%) were purchased from Aladdin Inc. NaOH was purchased from Macklin Inc. ethanol absolute(99.7%) and N-hexane(97.0%) were purchased from Sinopharm Chemical Reagent Co., Ltd.

2.2. Synthesis of CIZS QDs

CIZS QDs were synthesized in aqueous solution via a hydrothermal synthesis method. In a typical experiment, $CuCl_2 \cdot 2H_2O$(0.0125 mmol), $InCl_3 \cdot 4H_2O$(0.125 mmol) and $Zn(AC)_2 \cdot 2H_2O$ (0.0625 mmol) were dissolved in deionized water (15 mL), then GSH (0.875 mmol) was injected into the solution. The pH value of the mixture solution was adjusted to 11 by adding 2.0 $mol \cdot L^{-1}$ NaOH solution with stirring. During this process, the solution changed from turbid to clear pink. In the meantime, C_2H_5NS (0.875 mmol) was dissolved 1 mL deionized wate. After ultrasound for 10 minutes, C_2H_5NS was rapidly injected into the prior mixed solution. All the above mentioned experimental procedures were performed at room temperature. After vigorous stirring for 6 minutes, the solution was transferred into a Taflon-lined stainless steel autoclave with a volume of 25 mL. The autoclave was maintained at 120 °C for 4 h and then cooled down to room temperature by a natural cooling process. The CIZS QDs powder could be precipitated by ethanol absolute, and the precipitate was isolated by centrifugation, washed with ethanol absolute and N-hexane several times, then the CIZS QDs were obtained.

2.3. Cellular imaging

The ability and facility of the synthesized CIZS QDs for cellular imaging were evaluated by the fluorescence imaging of MDA-MB-231 cells. MDA-MB-231 cells were seeded in a 24-well plate at 37 °C for 24 h. The concentration of CIZS QDs solution for cellular imaging was 0.0625 $mg \cdot mL^{-1}$. The cells were treated with the CIZS QDs solution for another 24 h, followed by washed with PBS for three times. The fluorescence images were acquired by a fluorescent microscope (Olympus, IX71) under UV excitation with a peak at ~340 nm.

2.4. Characterization

XRD data were obtained on a Bruker D8 Advance X-ray diffractometer using Cu-Kα irradiation at λ = 0.15418 nm. TEM images were recorded on a Hitachi H-7650 electron instrument. FTIR spectra were recorded in 400~4000 cm^{-1} on a Nicollet 380 spectrophotometer using a KBr pellet. UV-Vis absorption spectra were obtained using a Shimadzu UV-2550 spectrometer. Photoluminescence (PL) measurements were carried out at room temperature with a Shimadzu RF-5301PC spectrofluorometer.

3. Results and discussion

3.1. Structural characterization

Fig. 1(a) showed the XRD patterns of GSH capped CIZS QDs. Three obvious diffraction peaks were located at 27.7°, 47.3°, and 55.5°, show a slight shift toward higher angles compared with the (112), (204), and (312) planes of chalcopyrite CuInS2 (JCPDS 27-0159) due to the decrease of the lattice constant, related to the incorporation of the smaller radius Zn^{2+} into the crystal lattice, indicating the formation of Cu–In–Zn–S alloyed structure[23]. The broad diffraction peaks of CZIS were due to the small size of QDs.

Fig. 1(b) showed the FT–IR spectra of GSH and GSH capped CZIS QDs synthesized at 120 °C for 4 h with the Cu/In molar ratio of 1:10. The peaks locked at 3022 cm^{-1} , 3249 cm^{-1} , 3346 cm^{-1} and 3126cm^{-1} of GSH were attributed to the N–H and C–O stretching vibration. The disappearance of the two peaks at 1536 cm^{-1}and2525 cm^{-1}, ascribed to the –NHR deformation vibration and–SH stretching vibration, indicating that the GSH was combined into the surface of CZIS QDs. Moreover, the peaks of anti-symmetrical stretching vibration of the–COO^- group were shifted from 1599 cm^{-1} to 1613 cm^{-1} , while the peak related to the symmetrical stretching vibration was shifted slightly from 1396.12 cm^{-1} to 1396.26 cm^{-1} .These results demonstrated that CZIS QDs were also functionalized with the–COO^- group of GSH. Therefore, the CZIS QDs coordinated with the GSH could well passivate surface defects, resulting in the effective improvement of the fluorescence property.

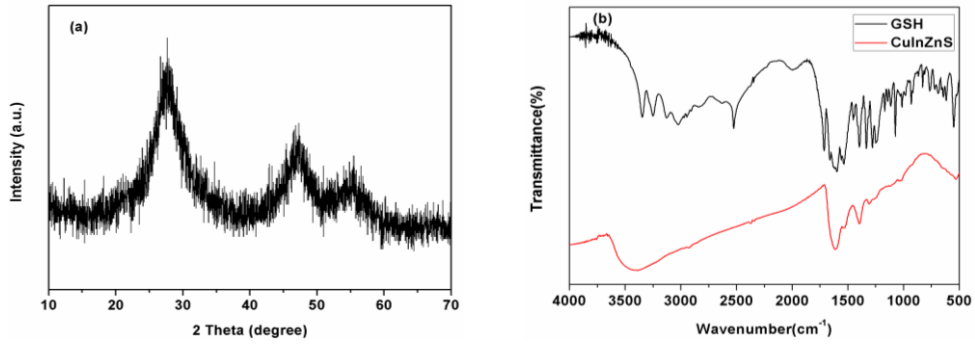

Fig. 1. XRD (a) patterns of GSH capped CIZS QDs prepared under optimum experimental conditions FT-IR(b) spectra of pure GSH(Top) and GSH-capped CIZS QDs(Bottom).

Fig. 2 (a) showed the TEM images of GSH capped CIZS QDs prepared under optimum experimental conditions. It is obvious that CIZS QDs are near-spherical shape and well-dispersed. Fig. 2 (b) displayed size distribution histograms of CIZS QDs and the mean particle size was 2.55 nm. The size distribution histograms were obtained from the TEM images. The inset in Fig.2(a) shown the digital camera of the CIZS QDs, from which it could be seen that the CIZS QDs emit strong orange fluorescence under the irradiation of 365 nm UV lamp and is yellow under daylight irradiation.

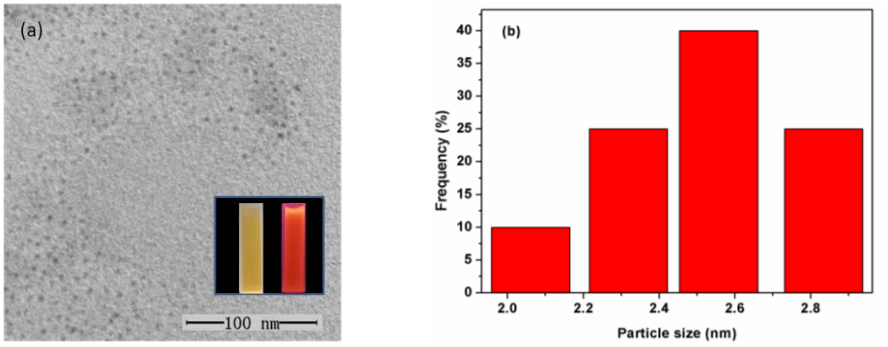

Fig. 2. TEM images (a) and size distribution (b) of GSH capped CIZS QDs under optimum experimental conditions.

3.2. Influence of reaction time

In order to study the effect of reaction time on the formation of GSH capped CIZS QDs, the corresponding precursors were heated at 120°C for different time. Fig. 3 showed typical absorption spectra and PL spectra of CIZS QDs with different reaction time. The absorption spectra of temporal evolution showed that there was no change in absorption onset, which indicated that the CIZS QDs have already formed in 3h (Fig.3 (a)). On the contrary, the PL intensity of the CIZS QDs was enhanced with increasing the reaction time, and reached to maximum under 4 h, followed by decrease gradually(Fig. 3 (b)).

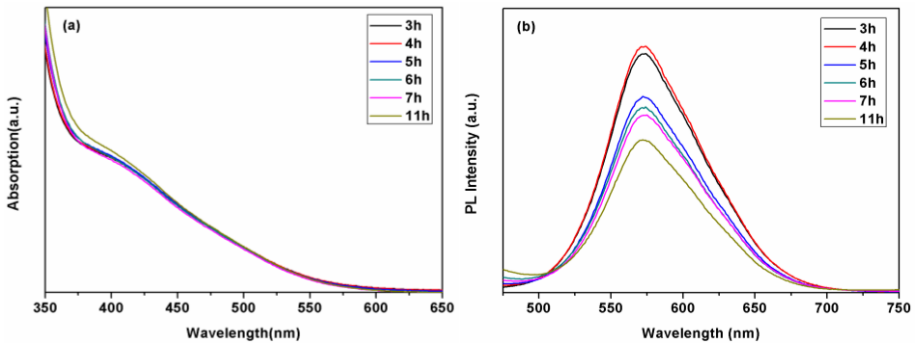

Fig. 3. The absorption spectra (a) and PL spectra (b) of GSH capped CIZS QDs under different reaction time.

It should be noted that there was almost no shift for wavelength peak of the CIZS QDs obtained under different reaction time, which further demonstrated that the formation of CIZS QDs have already formed in 3h, staying in consistent with the absorption spectra and indicating that extension of the reaction time do not enlarge the particle size. The increase in PL intensity may be attributed to better passivation of surface defects by the ligands, while the decrease could be explained by hydrolysis of the thiols, thus resulting in inadequate ligands to stabilize the system and to passivate the surface of the CIZS QDs. On the other hand, the structureless absorption spectra are observed, which are the typical indicative features of quaternary compounds, caused by the synergetic effect of the wide size distribution and the irregular composition distribution among different CIZS QDs. Such phenomena gived a clear indication that the PL emission was assigned to the radiative recombination of intrinsic defect–related states (donor-acceptor pairs) instead of band edge emission.

3.3. Influence of the pH value

Fig. 4(a) showed the PL spectra of GSH capped CIZS QDs prepared under under different pH value. It could be obviously observed that the PL spectra displayed a trend of the first ascent and then descent with increasing the pH value, and that the maximum PL intensity was obtained when the pH value is 11. Such maximum might be ascribed to stronger binding forces between GSH and the cations at this pH value. On the other hand, emission peak shifted from 596 nm to 560 nm with increasing the pH value.

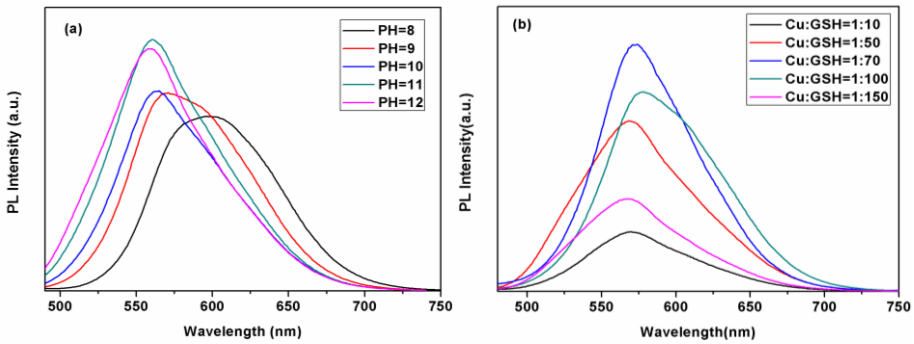

Fig. 4. The PL spectra (a) of GSH capped CIZS QDs under different pH value and the PL spectra (b) of GSH capped CIZS QDs under different Cu/GSH molar ratios.

3.4. Influence of Cu/GSH molar ratio

The addition of GSH to the reaction system plays an important role in the synthesis of CIZS QDs. GSH effect of reaction solution on the PL spectra were evaluated as displayed in Fig. 4(b) It could be obviously observed that the PL displays a trend of the first ascent and then descent with increasing GSH content, and that the maximum PL intensity is obtained when the molar ratio of GSH/Cu of 70/1. According to the previous report, there should be enough GSH in the system for passivating the nanoparticle surface and stabilizing the CIZS QDs. However, excess ligand might distort the surface, thus originating new nonradiative defects, which possibly accounted for the tendency in the experiments.

3.5. Influence of Cu/In molar ratio

Fig. 5 showed the PL spectra of GSH capped CIZS QDs under different Cu/In ratios. the PL intensity was gradually increased and then decreased with the molar ratio of Cu/In varying from 1/4 to 1/16, reaching a maximum value at Cu/In = 1/10. Based on the previous researches of defect states, the Cu-S bonds were much weaker than In-S bonds, causing Cu vacancies and In substitutions preferentially occurred[24]. In this case, S vacancies and substitutional In sites act as donors, in contrast, Cu vacancies act as acceptors. With the decrease of Cu/In mole ratio, the number of Cu vacancies increased gradually, which was beneficial to the enhancement of the recombination rate of CIZS QDs, so the PL intensity increased gradually. In addition, as the Cu/In mole ratio continued to decrease, the concentration of donor substitutional In and acceptor Cu vacancies In CIZS QDs decreased when Cu^{+} concentration was below the critical value, which leaded to the decrease of fluorescence intensity.

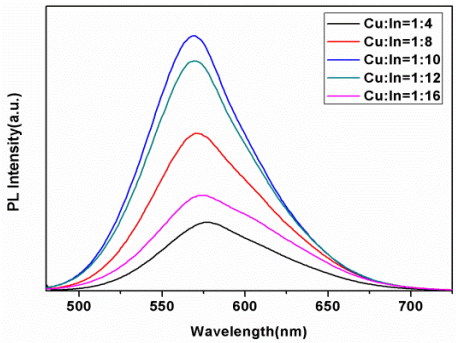

Fig. 5. The PL spectra of GSH capped CIZS QDs under different Cu/In molar ratios.

3.6. Cell labeling

Fig. 6 showed differential interference contrast (DIC) picture and fluorescent image of MDA-MB-231 cells incubated with GSH capped CIZS QDs. As showed in Fig.6 (b), the red emission CIZS QDs from the cells was clearly observed under fluorecent micoscope, which suggested that the GSH capped CIZS QDs can successfully enter into the MDA-MB-231 cells. This phenomenon showed that the QDs can perform as biomarkers for cancer cell fluorescence imaging. Compared with cadmium containing QDs, the toxicity of CIZS QDs was much less and therefore had more advantages for future clinical applications.

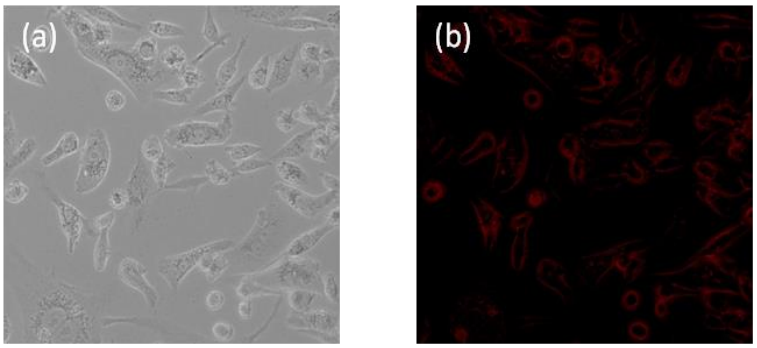

Fig. 6. Differential interference contrast (DIC) picture (a) and the fluorescent image (b) of MDA-MB-231cells labeled.

4. Conclusions

In summary, we report a one-pot method to directly synthesize highly luminescent CIZS QDs in aqueous media by using bio-compatible GSH as capping ligand and stabilizer. By changing the reaction time, the pH value, and the molar ratios of initial precursors, the influences of experimental variables on the optical properties were evaluated. When the molar ratio of Cu: In : Zn : S : GSH is 1 : 10 : 5 : 70 : 70 with reaction time 4 h and pH value 11, respectively. Compared with the traditional synthetic method in an organic solvent, this method was green, simple, and low cost. The prepared GSH capped CIZS QDs showed extremely water solubility and photostablity. Due to their unique and stable optical properties, the GSH capped CIZS QDs can be used in the areas of biomedical applications as a novel type of fluorescent nanoprobe.

Acknowledgments

This work was financially supported by the Scientific Research Foundation from Education Department of Heilongjiang Province (No. 2018-KYYWF-0086)

References

[1] A. P. Alivisatos, Science **271**, 933 (1996).
[2] X. G. Peng, L. Manna, W. D. Yang, J. Wickham, E. Scher, A. Kadavanich, A. P. Alivisatos, Nature **404**, 59(2000).
[3] L. L. Xi, H. B. Ma, G. H. Tao, Chin Chem Lett **27**, 1531 (2016).
[4] D. Kim, D. H. Kim, J. H. Lee, J. C. Grossman, Phys Rev Lett **110**, 196802 (2013).
[5] G. F. Wang, A. X. Guan, C. Y. Zhou, S. Y. Xia, Q. Chen, X. T. Chen, L. Y. Zhou, Chin Chem Lett **27**, 1788(2016).
[6] A. M. Derfus, W. C. W. Chan, S. N. Bhatia, Nano Letters **4**, 11 (2003).
[7] L. Lai, J. C. Jin, Z. Q. Xu, Y. S. Ge, F. L. Jiang, Y. Liu, Journal of Membrane Biology **248**, 727 (2015).
[8] L. J. Zhang, H. F. Yu, W. Cao, Z. Chao, Micro & Nano Letters **9**, 55 (2014).
[9] Y. W. Lan, K. Yang, Y. L. Wang, H. M. Li, Micro & Nano Letters **9**, 202 (2014).
[10] D. W. Deng, L. Z. Qu, J. Zhang, Y. X. Ma, Y. Q. Gu, Appl Mater Interfaces **5**, 10858 (2013).
[11] W.G Kong, B. P. Zhang, R. F. Li, F. F. Wu, T. N. Xu, H. Z. Wu, Appl Surf Sci **327**, 394 (2015).
[12] Y. Wang, Y. X. Hu, Q. Zhang, J. P. Ge, Z. D. Lu, Y. B. Hou, Y. D. Yin, Inorg Chem **49**, 6601 (2010).
[13] P. L. Saldanha, R. Brescia, M. Prato, H. Li, M. Povia, L. Manna, V. Lesnyak, Chem Mater **26**, 1442 (2014).
[14] T. Torimoto, T. Adachi, K. I. Okazaki, M. Sakuraoka, S. Kuwabata, J Am Chem Soc **129**, 12388 (2007).
[15] D. Aldakov, A. Lefrancois, P. Reiss, J Mater Chem C **1**, 3756 (2013).
[16] O. Yarema, D. Bozyigit, I. Rousseau, L. Nowack, M. Yarema, W. Heiss, V. Wood, Chem Mater **25**, 3753 (2013).
[17] W. D. Xiang, X. Ma, L. Luo, W. Cai, C. P. Xie, X. J. Liang, Mater Chem Phys **149-150**, 437 (2015).
[18] H. Nakamura, W. Kato, M. Uehara, K. Nose, T. Omata, Chem Mater **18**, 3330 (2006).
[19] W. Y. Liu, Y. Zhang, W. W. Zhai, Y. H. Wang, T. Q. Zhang, P. F Gu, H. R. Chu, H. Z. Zhang, T. Cui, Y. D. Wang, J. Zhao, William, W. Yu, J Phys Chem C **117**, 19288 (2013).
[20] W. J. Zhang, X.H. Zhong, Inorg Chem **50**, 4065 (2011).
[21] L. Ding, P. J. Zhou, H. Zhan, C. Chen, W. Hu, T. F. Zhou, C. W. Lin, Journal of Luminescence **142**, 167 (2013).

[22] Y. Zheng, S. Gao, J. Y. Ying, Adv Mater **19**, 376 (2007).
[23] Z. S. Leng, L. Huang, F. Shao, Z. C. Lv, T. T. Li, X. X. Gu, H. Y. Han, Mater Lett **119**, 100 (2014).
[24] W. Y. Mao, J. Guo, W. L. Yang, C. C. Wang, J. He, J. Y. Chen, Nanotechnology **18**, 485611 (2007).